Developmental Biology 455 (2019) 73–84

Contents lists available at ScienceDirect

Developmental Biology

journal homepage: www.elsevier.com/locate/developmentalbiology

Original research article

Loss of flow responsive Tie1 results in Impaired Aortic valve remodeling

Xianghu Qu [a,1], Kate Violette [b,1], M.K. Sewell-Loftin [c], Jonathan Soslow [a], LeShana Saint-Jean [b], Robert B. Hinton [d], W. David Merryman [c], H. Scott Baldwin [a,b,*]

[a] Division of Pediatrics Cardiology, Vanderbilt University, Nashville, TN, USA
[b] Department of Cell and Developmental Biology, Vanderbilt University, Nashville, TN, USA
[c] Department of Biomedical Engineering, Vanderbilt University, Nashville, TN, USA
[d] Division of Cardiology, The Cincinnati Children's Hospital Medical Center, Cincinnati, OH, USA

ARTICLE INFO

Keywords:
Semilunar valves
Endocardium
Extracellular matrix
Hemodynamics
Sox9

ABSTRACT

The mechanisms regulating endothelial cell response to hemodynamic forces required for heart valve development, especially valve remodeling, remain elusive. Tie1, an endothelial specific receptor tyrosine kinase, is up-regulated by oscillating shear stress and is required for lymphatic valve development. In this study, we demonstrate that valvular endothelial Tie1 is differentially expressed in a dynamic pattern predicted by disturbed flow during valve remodeling. Following valvular endocardial specific deletion of Tie1 in mice, we observed enlarged aortic valve leaflets, decreased valve stiffness and valvular insufficiency. Valve abnormalities were only detected in late gestation and early postnatal mutant animals and worsened with age. The mutant mice developed perturbed extracellular matrix (ECM) deposition and remodeling characterized by increased glycosaminoglycan and decreased collagen content, as well as increased valve interstitial cell expression of Sox9, a transcription factor essential for normal ECM maturation during heart valve development. This study provides the first evidence that Tie1 is involved in modulation of late valve remodeling and suggests that an important Tie1-Sox9 signaling axis exists through which disturbed flows are converted by endocardial cells to paracrine Sox9 signals to modulate normal matrix remodeling of the aortic valve.

1. Introduction

Heart valve defects are among the most common human congenital anomalies, with an incidence of approximately 2% of live births (Hoffman and Kaplan, 2002; van der Linde et al., 2011). In the mouse embryo, the anlages of the mature valves are first evident as swellings termed endocardial cushions in the atrioventricular (AV) canal and outflow tract (OFT) around embryonic day 9 (E9), and these swellings function to prevent retrograde flow through the heart. Endocardial cells in the cushion undergo an endothelial to mesenchymal transformation (EMT) to initiate formation of the mitral and tricuspid valves and somewhat later in the OFT to initiate formation of the aortic and pulmonary valves (for review, see DeLaughter et al., 2011; Lin et al., 2012). Following EMT, the valves elongate and are remodeled into thin, mature valve leaflets, a process which continues through late gestation, after birth and into the juvenile period (Aikawa et al., 2006; Hinton et al., 2006). Although the early processes of EMT and cushion formation have been studied in some detail, mice with defects in EMT rarely survive to birth (reviewed in von Gise and Pu, 2012). Increasing evidence suggests that viable valve disease in humans is associated with dysregulation of signaling events in latter stages of valve remodeling which are poorly understood. Some congenital valve defects have been linked to specific genetic mutations, such as NOTCH1, TBX5, GATA4 and TBX20; however, most have no clearly definable genetic or environmental cause (Garg et al., 2005; Levine et al., 2015).

Increasing evidence from chicks and zebrafish suggests that hemodynamic forces play an essential epigenetic role in heart valve development. However, the molecular pathways by which blood flow and shear forces regulate heart valve development, particularly in mammals, are poorly delineated. Valve endothelial cells (VECs) on the aortic valve (AoV) surfaces are exposed to shear stresses during every cardiac cycle. The ventricular side of the valve is exposed to high laminar shear stress.

* Corresponding author. 9435-A MRB IV/VUMC, Nashville, TN, 37232- 0493, USA.
E-mail address: scott.baldwin@vumc.org (H.S. Baldwin).
[1] These authors made equal contributions to this manuscript.

https://doi.org/10.1016/j.ydbio.2019.07.011
Received 13 March 2019; Received in revised form 11 July 2019; Accepted 14 July 2019
Available online 15 July 2019

In contrast, the aortic side of the valve is exposed to oscillatory shear stress. Endothelial cells from each side of the valve have unique transcriptional profiles (Simmons et al., 2005). Both laminar and oscillatory shear forces may have important roles in regulating normal heart valve development. For example, the transcription factors KLF2 and KLF4, up-regulated by laminar shear stress and specifically expressed in the VECs on the ventricular side of the developing valve, are required for cardiac cushion formation and regulate the mesenchymal cell responses that remodel cardiac cushions to mature valves (Chiplunkar et al., 2013; Goddard et al., 2017). In contrast, oscillatory shear stress activates the expression of Foxc2, ephrin-B2, and Tie1 (Woo et al., 2011) in ECs. Consistent with these observations, expression of Foxc2, ephrin-B2 and CX37 is enriched on the aortic side of the AoV (Gitler et al., 2003; Cowan et al., 2004; Inai et al., 2004). ephrin-B2 was identified as an artery-specific marker (Gerety et al., 1999). Loss of the cytoplasmic domain of ephrin-B2 results in thickened cardiac valves (Woo et al., 2011).

Tie1 is an orphan endothelial receptor tyrosine kinase sharing a high degree of homology with Tie2, the receptor for the angiopoietins (Yancopoulos et al., 2000). It is expressed throughout both the blood and lymphatic vasculature endothelium from early embryonic stages to adulthood (Dumont et al., 1995; Puri et al., 1995; Qu et al., 2010). The expression of Tie1 is markedly attenuated in the postnatal vasculature with the exception of persistent expression on the arterial side of the AoV leaflets as well as branch points of the descending aorta (Porat et al., 2004; Woo et al., 2011). Prior studies by us (Woo et al., 2011) and others (Porat et al., 2004; Zheng et al., 2004) have demonstrated that Tie1 expression is up-regulated by turbulent flow in cultured human endothelial cells, mouse primary aortic ECs, and mouse vascular endothelium *in vivo*. Tie1 is at least partially responsible for mechanotransduction of disturbed flow required for initiation and maintenance of atherosclerotic plaque formation at the branch points of the systemic vasculature in the adult animal (Woo et al., 2011). In addition, we have previously shown that Tie1 is required for lymphatic vessel remodeling and lymphatic valve formation (Qu et al., 2015). However, its potential roles in heart valve development have not been explored. In the present study, we show accentuated expression of Tie1 on the arterial side compared to the ventricular side of semilunar valves in the late gestation embryo. This accentuated expression pattern correlates with the increasing oscillatory shear forces during late valve remodeling. Deletion of Tie1 specifically in the developing valvular endocardium resulted in an expansion of AoV size, with perturbations in ECM production and stratification leading to structural and functional deficits in postnatal mice. Abnormal valve development in *Tie1* mutants was accompanied by increased valvular interstitial cell (VIC) expression of Sox9, a transcription factor essential for normal remodeling of valve ECM (Lincoln et al., 2007). Localization of Sox9 expression to the ventricular side of the aortic valve normally seen with maturation was perturbed, resulting in ubiquitous distribution of Sox9 and subsequent arrest of valve remodeling. Our studies suggest a VEC Tie1-VIC Sox9 signaling axis through which disturbed flow are converted by endocardial cells to paracrine Sox9 signals that modulate the remodeling of the AoV. These findings suggest a significant role for Tie1 in modulation of late valve remodeling and early postnatal valve maintenance that has not been previously appreciated.

2. Materials and methods

2.1. Mice

Generation of *Tie1*$^{+/lz}$(Puri et al., 1995), *Tie1*$^{fl/fl}$(Qu et al., 2010), and *Nfatc1*^{en}*Cre* mice (Wu et al., 2011), has been described previously. R26R reporter (*R26*^{fslz}) mice were purchased from The Jackson Laboratory (Bar Harbor, ME). For BrdU incorporation, pregnant females were injected intraperitoneally with BrdU (Roche Diagnostics) at a dosage of 10 μl per gram bodyweight. After 2 h, mice were sacrificed and embryos were fixed in 4% PFA in PBS. All strains were maintained on a mixed 129 and C57/BL6 background. The animals were handled in accordance with institutional guidelines with the approval of the Institutional Animal Care and Use Committee of Vanderbilt University School of Medicine.

2.2. X-gal staining

Embryos, embryonic or postnatal hearts were whole-mount stained with X-gal as described (Qu et al., 2015). In short, freshly dissected embryos or hearts were fixed in glutaraldehyde, and whole embryos or hearts were stained overnight and processed for paraffin embedding. X-gal staining was performed on frozen sections as described (Qu et al., 2010). Briefly, cryoprotected embryos were embedded in OCT (Tissue Tek) and cryosectioned, stained for β-galactosidase (β-gal) activity, and then immuno-stained with primary antibody goat anti-Tie2 (R&D Systems) and fluorescently labeled secondary antibody.

2.3. Histology and immunohistochemistry

Standard histological procedures were used. Embryonic, postnatal and adult tissues were fixed in 4% paraformaldehyde, embedded in paraffin or OCT and sectioned at 6 or 10 μm. Paraffin sections were stained with Hematoxylin and Eosin (H&E), Movat's Pentachrome stain (Poly Scientific), or subjected to an immunostaining. The primary antibodies that were used for immunostainings of paraffin or frozen sections are listed in the Key Resource Table. All secondaries for immunofluorescence were AlexaFluor labeled (Thermo Fisher Scientific), except NL557 conjugated donkey anti-sheep IgG (R&D Systems, NL010, 1:600). To detect apoptosis in semilunar valves, the TUNEL assay was carried out using ApopTag Plus Fluorescein *in situ* Cell Death Detection Kit (CHEMICON International, S7111). Images were visualized with an Olympus BX60 microscope and captured using Advanced SPOT image software. To quantify expression from immunohistochemical data, digital images of heart valve sections were acquired at identical confocal settings, and then the positive pixels were measured using NIH Image J and normalized to total tissue area (Goddard et al., 2017). Ultrastructural analysis of endothelial morphology was examined with transmission electron microscopy (EM) as described (Odelin et al., 2014).

2.4. Quantification of size and cell numbers of valves

Valve morphometry was assessed on H&E stained sections as previously described using NIH Image J (Hinton et al., 2008). Briefly, valve area was measured from the annulus to the tip, and valve thickness was measured by the widest portion of the cusps or leaflets of valves over a minimum depth of 50 μm. Sequential sections were reviewed and measurements were obtained from representative sections. Three sections were measured in triplicates and averaged from six mice per genotype for statistical analysis. For quantification of valvular cell numbers, the total nuclei in the valve cusps were counted in DAPI stained sections spanning a depth of at least 50 μm. 5–8 consecutive sections from each mouse and 5 animals per genotype per age group were measured.

2.5. Quantitative RT-PCR

Quantitative PCR was performed on the LightCycler (Roche) using the LightCycler DNA Master SYBR Green I Kit (Roche) with a *Gapdh* control. Primer sets for *Tie1* (Dumont et al., 1995) and *Col1a1*, *Col1a2* and *Col3a1* (Odelin et al., 2014) have been published previously. All assays were repeated three times, and all samples were run in triplicate. Level changes were calculated by the comparative cycle threshold (ΔΔCT) method.

2.6. ECM measurements

Soluble collagen in valve leaflets was measured using the Sircol Soluble Collagen Assay (Biocolor Ltd.). Aortic valve leaflets were dissected

away from the vessel. AoVs from 3 animals were pooled for each sample. A total of 4 samples for each genotype was measured with a microplate reader. Glycosoaminoglycans (GAGs) in valve leaflets were measured using the Blyscan Sulfated Glycosaminoglycan Assay (Biocolor Ltd.). Valve leaflets (n=12) were pooled per sample for each genotype, and all samples were performed in triplicate.

2.7. Atomic force microscopy technique

To quantify valve leaflet mechanical properties, an atomic force microscope (Bruker AXS, Madison WI, USA) was utilized in Peak Force Quantitative Nanomechanical Mapping (PF-QNM) mode, which is a modified tapping mode (Sewell-Loftin et al., 2012). Sample modulus (E) is calculated by the NanoScope Analysis software in the following equation:

$$F_{tip} = \frac{4}{3}E\sqrt{Rd^3} + F_{adh}$$

where F_{tip} is the force on the tip, R is the radius of the tip, d is the distance between sample and tip, and F_{adh} is the adhesive force between the sample and tip. The Poisson ratio, v, is set at 0.5. For all analyses, borosilicate glass particle tips (Novascan Technologies, Inc., Ames IA, USA) with a nominal radius of 2.5 μm and spring constant of 0.03 N/m were utilized. Tips were calibrated prior to sample analysis using in house made poly(dimethylsiloxane) (PDMS) standards.

Aortic valve samples at two month old for AFM analysis were prepared by flash freezing in OCT without fixation, sectioned at 10 μm, and stored at −20 °C until use. Each samples wash cleared of OCT by washing in PBS, then stained for 30 min at room temperature with 1:300 each Cy3 alpha-smooth muscle actin (C6198 Sigma, St. Louis MO, USA) and FITC CD31 (558738 BD Pharminigen, San Diego CA, USA) diluted in Hank's buffered salt solution containing 0.2% FBS and 0.1 μg/mL DAPI. Slides were washed 3X in PBS, rinsed in diH2O before analysis. All samples were scanned either at 20 x 20 μm or 30 x 30 μm, with sizes varied to ensure alignment of AFM data with topographical features. Areas were scanned at 0.1 Hz with peak force setpoints between 0.1-1 nN, based on calibration parameters. For AV leaflet sections, a minimum of 2 adjacent areas were scanned and multiple sections and animals (n = 3 per group) were used.

2.8. Echocardiograms

Postnatal mice were sedated with isoflurane, restrained and placed on a heated table with a continuous isoflurane anesthesia as previously described (Hinton et al., 2008). Embryonic mice were studied at E17.5 following laparotomy of the anesthetized pregnant mother, exposure of the uterine horn and serial transthoracic evaluation of the individual fetuses. All studies were performed with a VisualSonics Vevo 2100 using the MS-400 probe (18–38 MHz). 2-dimensional imaging was obtained in the long axis, short axis, apical 4-chamber, and aortic arch views. Pulsed wave Doppler and color flow mapping was used to assess for insufficiency of the semilunar and atrioventricular valves, and Pulsed wave Doppler was used to assess for valvar dysfunction (stenosis and/or insufficiency). M-mode measurements were performed in short axis to assess ventricular function and chamber dimensions.

2.9. Statistics

Data were analyzed with GraphPad Prism (version 7) and represented as mean ± SD. P values were calculated using an unpaired, 2-tailed Student's t-test. A p value < 0.05 was considered statistically significant.

2.10. Key Resource Table (antibodies for IHC)

Antibodies		SOURCE	IDENTIFIER	Working concentration
Rabbit anti-pHH3		Upstate	Cat#06–570; PRID: AB_310177	1:100
Rat anti-BrdU		Abcam	Cat#ab6326; PRID: AB_305426	1:100
Rabbit anti Cleaved Caspase-3 (Asp175)		Cell Signaling	Cat#9664; PRID: AB_2070042	1:400
Goat anti Tie1		R&D Systems	Cat#AF619; PRID: AB_355481	1:50
Goat anti-mouse Tie2	R&D Systems	Cat#AF762; PRID:AB_2203220	1:400	
Rat anti-mouse CD31	Pharmingen,	Cat#557355; PRID:AB_396660	1:200	
Mouse anti Collagen III	Abcam	Cat#ab6310; PRID:AB_305413	1:400	
Rabbit anti Collagen I	Abcam	Cat#ab34710; PRID:AB_731684	1:100	
Rabbit anti-Erg1	Abcam	Cat#ab92513; PRID:AB_2630401	1:100	
Goat anti-VE-Cadherin	R&D Systems	Cat#AF1002; PRID:AB_2077789	1:400	
Rabbit anti-Versican (GAGβ)	Chemicon	Cat#AB1033; PRID:AB_90462	1:1500	
Hyaluronic acid binding protein, biotinylated (HABP)	Millipore	Cat#385911	1:100	
Goat anti-Sox9	Cell Signaling	Cat#82630	1:100	
Rabbit anti Versican V0,V1 Neo (DPEAAE)	ThermoFisher	Cat#PA1-1748A; PRID:AB_2304324	1:1500	
Sheep anti-Foxc2	R&D Systems	Cat#AF6989; PRID:AB_10973139	1:200	
NL557 Conjugated donkey anti-sheep IgG	R&D Systems	Cat#NL010; PRID:AB_884220	1:600	

3. Results

3.1. Valvular endothelial Tie1 is expressed in a progressively graded pattern predicted by disturbed shear stress during valve remodeling

Tie1 is expressed in the valve endothelial cells, and its expression on the arterial side (predicted to be exposed to reversing oscillatory shear stress) of the semilunar valve leaflet is higher than that on the ventricular side (predicted to be exposed to high laminar shear stress) in the adult (Dumont et al., 1995; Puri et al., 1995; Woo et al., 2011). However, the time window when this polarized expression pattern is initiated and its potential role in heart valve development have not been explored. To further characterize Tie1 expression and make a comparison with other flow sensitive endothelial markers (CD31, Cdh5 and Tie2) in the developing semilunar valves, we performed immunohistochemical analysis at sequential stages of *in utero* development (Fig. 1). Consistent with prior studies, all of these cell surface proteins were ubiquitously expressed in the ECs lining the ventricular and arterial aspects of cardiac cushions or valve leaflets prior to E14.5 (data not shown). However, by E14.5, Tie2 begins to demonstrate accentuated expression in the arterial side of the valve leaflet (Fig. 1A, S1A), while Tie1, CD31 and Cdh5 are still evenly expressed on both the arterial and ventricular sides of semilunar valves. From E16.5, Tie1 and Cdh5 begin to have an accentuated level of expression on the arterial side of semilunar valves. In contrast, CD31

starts to show higher expression on the ventricular valve surface. This polarized expression pattern of these four EC markers is persistent and more significant at E18.5 and post-natal day 0 (P0) (Fig. 1B, C, S1B, C), as laminar shear forces on the ventricular side and disturbed forces on the arterial side are predicted to gradually increase. Quantitative analysis (Fig. 1F) revealed that between E14.5 and P0, relative expression of Tie1 and Cdh5 on the arterial side vs. ventricular side progressively increased. In contrast, relative expression of CD31 on the arterial vs. ventricular progressively decreased, and Tie2 was detected almost exclusively on the ventricular valve surface in AoV or PV at P0. Utilizing the *Tie1*$^{+/lacz}$ reporter line (Puri et al., 1995), in which β-galactosidase expression is under the control of the endogenous *Tie1* regulatory elements, we further confirm polarized Tie1 expression in P0 semilunar valves by X-gal staining of *Tie1*$^{+/lacz}$ heart sections (Fig. 1D, E, S1D, E). These results demonstrate that Tie1 is expressed in a progressively restricted fashion in endothelial cells lining the arterial surfaces of cardiac valves, coincident with its known function in transducing endothelial cell responses to disturbed shear forces in the systemic vasculature (Dumont et al., 1995; Woo et al., 2011) and its role during the formation and remodeling of lymphatic valves (Qu et al., 2015).

3.2. Attenuation of Tie1 in the valvular endocardium results in enlarged AoVs from the late gestation

To specifically determine the role of Tie1 in valve development, we utilized a floxed *Tie1* allele (Qu et al., 2010) and a valvular endocardial specific Cre transgenic line (*Nfatc1*^{en}*Cre*) (Wu et al., 2011). We first analyzed Cre activity by X-gal staining of *R26*^{fslz};*Nfatc1*^{en}*Cre* heart sections, showing that Cre expression was restricted to the endothelium of the developing valves but not the endothelium of the artery or mesenchyme derived from EMT at E12.5, at E14.5 and at P0, and that *lacZ* expression persists in the majority of the valvular endothelial cells through adulthood (Fig. 2A–D). We crossed *Tie1*$^{fl/lz}$ mice, where *lacZ* is knocked in to the *Tie1* locus and produces a null allele, with *Tie1*$^{+/fl}$;*Nfatc1*^{en}*Cre* mice to generate valvular endocardial-specific *Tie1* knockout mice *Tie1*$^{fl/lz}$;*Nfatc1*^{en}*Cre*. Immuno-staining of semilunar valves with

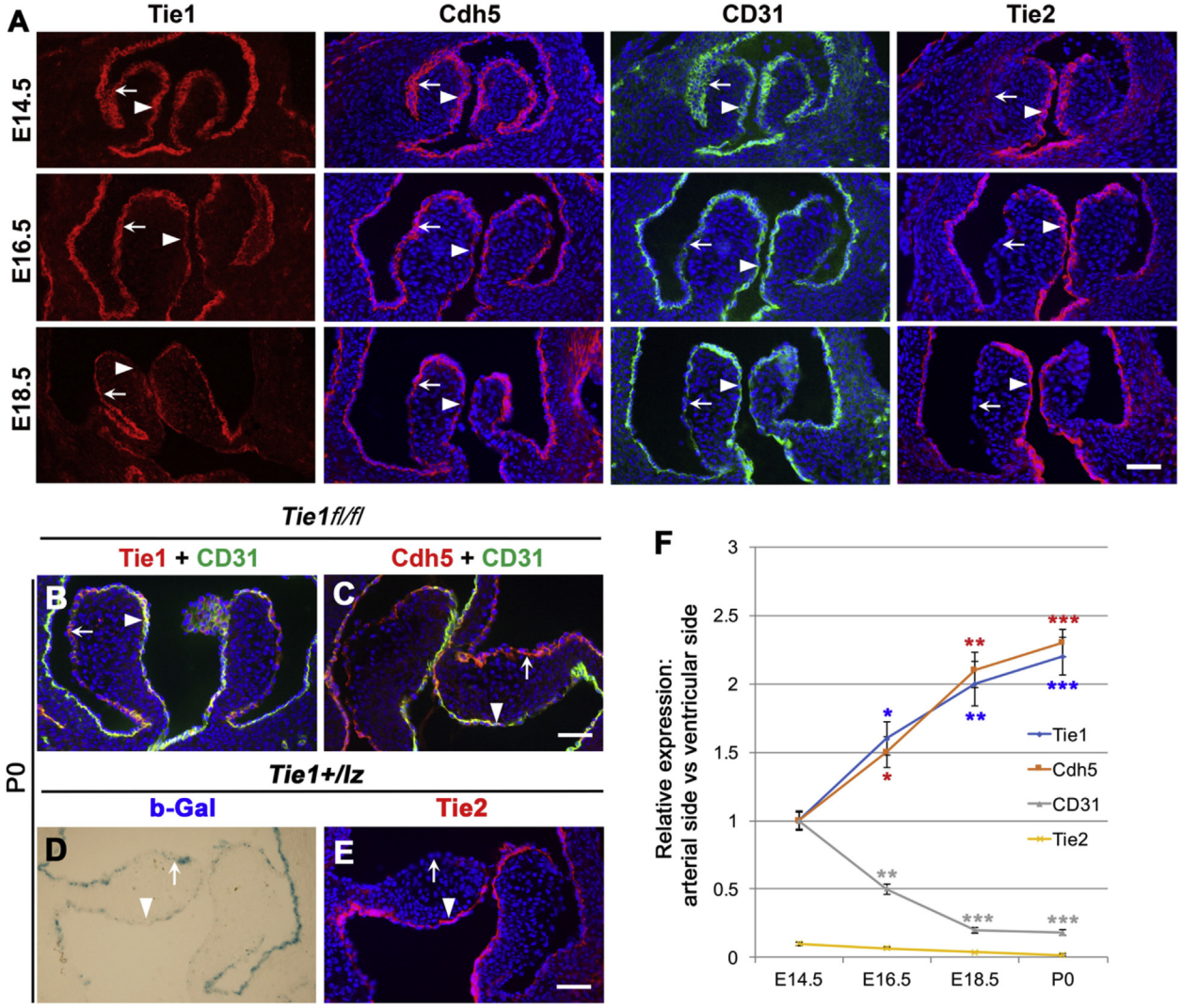

Fig. 1. Polarized expression of Tie1 and other flow sensitive endothelial markers in the remodeling aortic valves. **A**, Tie1 (red), Cdh5 (red), CD31 (green) and Tie2 (red) expression in remodeling aortic valves was detected by immunostaining *Tie1fl/fl* hearts at E14.5, E16.5, and E18.5. **B** and **C**, AoV sections of P0 *Tie1fl/fl* heart were coimmunostained for Tie1 (red) and CD31 (green) or Cdh5 (red) and CD31 (green). **D,** P0 *Tie1+/lacz* heart AoV sections were stained for (b-Gal, b-galactosidase) with X-gal (blue) and then with Tie2 antibody (red, **E**). DAPI (blue) denotes nuclei. Scale bars: 50 μm. From E16.5, Tie1 and Cdh5 begin to have higher expression on the arterial sides (arrows); in contrast, CD31 and Tie2 have higher expression on the ventricular sides (arrowheads). **F**, Quantification of relative expression of Tie1, Cdh5, CD31 and Tie2 in remodeling aortic valves: arterial side (predicted to face oscillatory shear stress) vs. ventricular side (predicted to face high laminar shear stress). $^{*}P < 0.05$, $^{**}P < 0.0,1^{***}P < 0.001$ (all compared with E14.5).

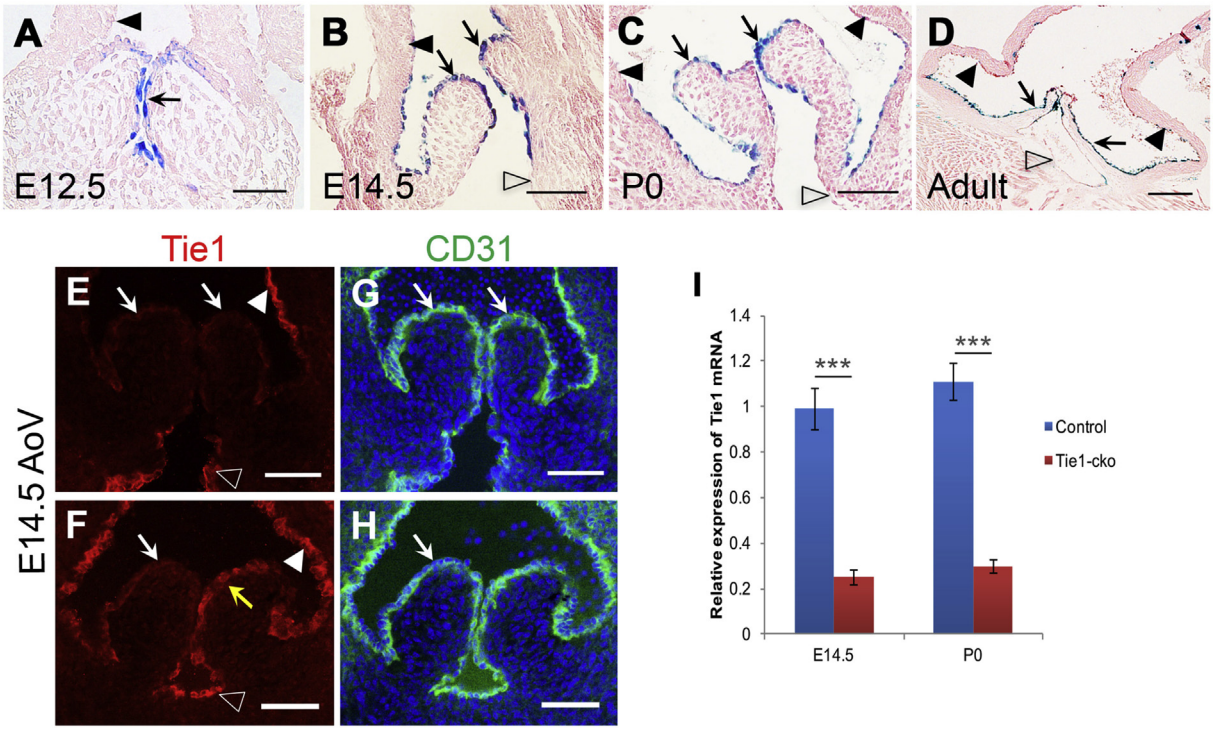

Fig. 2. *Nfatc1enCre* mediates *loxP* excision exclusively in the valvular endocardium. **AD**, X-gal staining of *R26fslz;Nfatc1enCre* heart sections shows that *Nfatc1enCre*-mediated recombination is restricted to the endothelium of the developing aortic valves (arrows) but not the endothelium of the artery (solid arrowheads), mesenchyme derived from EMT or ventricular endocardium (open arrowheads) at E12.5 (**A**), at E14.5 (**B**) and at P0 (**C**), and *lacZ* expression remains in the majority of the valvular endothelial cells throughout adulthood (**D**). **E**, Representative images of immuno-staining of *Tie2-cko* AoVs at E14.5 with anti-Tie1 antibody showing efficient specific Tie1 deletion in valvular endothelium (arrows) without change of normal expression of Tie1 in arterial endothelium (solid arrowheads) or ventricular endocardium (open arrowheads). **F**, *Nfatc1enCre*-mediated Tie1 deletion was not very efficient in a few (2 out of 9) mutant embryos. **G** and **H**, the same sections in **E** and **F** were co-stained for CD31, showing the integrity of endothelial cells. Yellow arrows indicate the mosaic Tie1 expression in the mutant valvular endothelium. DAPI, blue. Scale bars: 50 μm in A-C, H-I and 200 μm in D. **I**, The efficiency of Cre mediated Tie1 deletion in AoVs was assessed with qRTPCR on valve leaflets of *Tie1fl/fl* (control) and *Tie1fl/lz;Nfatc1enCre* (*Tie1-cko*) mice at E14.5 and at P0. For normalization, *Tie1* mRNA level in control mice at E14.5 was set as 1. $^{***}P < 0.001$.

anti-Tie1 antibody detected only minimal and sporadic Tie1 staining in the valvular endocardium without change of normal expression of Tie1 in arterial ECs or ventricular endocardium (Fig. 2E, S2A), confirming efficient and specific valvular Tie1 deletion in most *Tie1-cko* animals at E14.5 (78%, 7 out of 9) and at P0 (5 out of 7, data not shown). We occasionally observed sporadic Tie1 staining in a few endothelial cells of *Tie1-cko* semilunar valves (Fig. 2F, S2C), indicating small variations in the efficiency of *Nfatc1^{en}Cre* mediated *Tie1* deletion. Consistently, loss of expression of *Tie1* in *Tie1-cko* semilunar valves was 67%–77%, as determined by qRT-PCR on valve leaflets of *Tie1$^{fl/fl}$* (control) and *Tie1$^{fl/lz}$;Nfatc1^{en}Cre* mice at E14.5 and at P0 (Fig. 2I, S2E).

Many of the *Tie1$^{fl/fl}$;Nfatc1^{en}Cre* mice survived to adulthood and are fertile. Therefore, we were able to cross *Tie1$^{fl/lz}$* mice with *Tie1$^{fl/fl}$;Nfatc1^{en}Cre* mice and thus increase the efficiency of *Tie1* deletion by generation of *Tie1$^{fl/lz}$;Nfatc1^{en}Cre* mice. This cross is predicted to generate 25% of each of the following offspring: *Tie1$^{fl/fl}$*, *Tie1$^{fl/lz}$*, *Tie1$^{fl/fl}$;Nfatc1^{en}Cre* and *Nfatc1^{en}Cre;Tie1$^{fl/lz}$* (Table 1). In fact, the frequency of *Tie1$^{fl/lz}$;Nfatc1^{en}Cre* pups at P0 (13%) and at weaning (9%) is significantly lower than expected (25%), indicating that about half of the mutant mice died during the later stages of gestation or in the first days of life. Within a few days after birth, most *Tie1$^{fl/lz}$;Nfatc1^{en}Cre* and *Tie1$^{fl/fl}$;Nfatc1^{en}Cre* mutant pups could be distinguished from *Tie1$^{fl/fl}$* littermates, as the mutants are often growth retarded and lethargic, while 72% of *Tie1$^{fl/fl}$;Nfatc1^{en}Cre* mice and only 36% of *Tie1$^{fl/lz}$;Nfatc1^{en}Cre* mice survived to adulthood. If animals survived to adulthood, they appeared normal, viable and fertile. Thus, loss of *Tie1* in the valve endocardium reduces survival rates in a dosage-dependent manner. In all subsequent experiments, we utilized only *Tie1$^{fl/lz}$;Nfatc1^{en}Cre* mice as *Tie1* mutant group (*Tie1-cko*, hereafter).

Histological analysis detected no difference in valvular morphology between the *Tie1-cko* and control (*Tie1$^{fl/fl}$* or *Tie1$^{fl/lz}$*) littermates before E16.5, indicating that early events of valvulogenesis occur normally in endocardial specific *Tie1* mutant mice. However, in the late gestational and postnatal mice, we observed an increase in aortic valve size in *Tie1-*

Table 1
Distribution and survival of *Tie1$^{fl/fl}$;Nfatc1^{en}Cre* X *Tie1$^{fl/lz}$* progeny during development. Crossing *Tie1$^{fl/lz}$* with *Tie1$^{fl/fl}$;Nfatc1^{en}Cre* resulted in the expected Mendelian distribution through E16.5, but reduced viability was detected at E18.5 as well as in the postnatal period.

Age	*Tie1$^{fl/fl}$* (%)	*Tie1$^{fl/lz}$* (%)	*Tie1$^{fl/fl}$; Nfatc1^{en}Cre* (%)	*Tie1$^{fl/lz}$;Nfatc1^{en}Cre* (%)	Total number
E14.5	61 (24)	63 (25)	60 (24)	68 (27)	252
E16.5	11 (28)	12 (30)	9 (22)	8 (20)	40
E18.5	15 (33)	13 (29)	10 (22)	7 (16)	45
P0	77 (34)	73 (32)	48 (21)	29 (13)	227
3 weeks	355 (36)	365 (37)	178 (18)	89 (9)	987
adult	299 (40.4)	307 (41.4)	108 (14.6)	27(3.6)	741

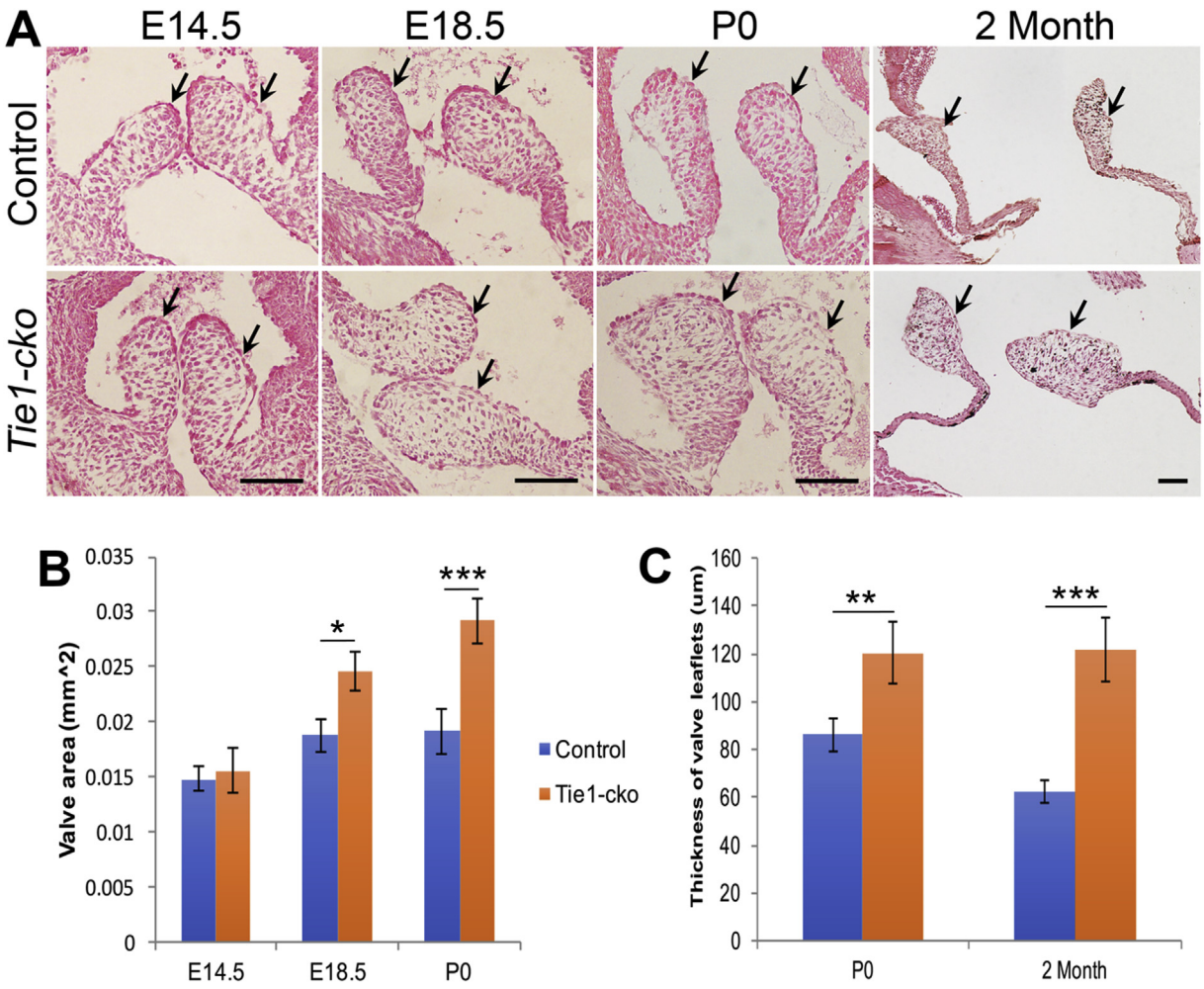

Fig. 3. Perinatal and adult *Tie1-cko* animals have enlarged aortic valves. **A**, H&Estained sections of AoVs (aortic valves) of *Tie1fl/fl*(control) and *Tie1-cko* mice at E14.5, at E18.5, at P0 and at adult (2 months) show increased AoV size in the mutants from E18.5. Arrows indicate valve leaflets. Scale bars: 50 μm. **B** and **C**, Quantitative analysis of size of AoVs from control and *Tie1-cko* mice at E14.5, at E18.5, at P0 and at adult. Values in (**B**) represent the average area of two valve leaflets in a field. Compared to controls, aortic valves of *Tie1-cko* mice are significantly larger from E18.5 to adulthood. $*P < 0.05$, $**P < 0.0,1***P < 0.001$.

cko animals compared to controls (Fig. 3A). The valve area of the mutant AoVs at E18.5 and P0 was increased by 30.7% and 54.5%, respectively (Fig. 3B). This trend continued through adulthood, when we observed that 71.4% (25 out of 35) of adult *Tie1-cko* mice had enlarged AoVs, nearly twice as large as control AoVs (increased by 94.7%) (Fig. 3C). 28.6% of *Tie1-cko* mice that survived into adulthood had normal AoVs. Interestingly, there was no difference in the size of the PVs (Fig. S3), tricuspid valves or mitral valves (data not shown) between *Tie1-cko* and control mice both before and after birth.

3.3. *Tie1 deficiency leads to decreased AoV stiffness and insufficiency*

To determine the potential alterations in the mechanical properties of the valve leaflet, we utilized atomic force microscopy (AFM) (Sewell-Loftin et al., 2012) to quantify the stiffness of valves from both control and *Tie1* mutant animals at two month old (Fig. 4). Stiffness of control valves using this methodology was comparable to that defined by an analysis utilizing a modified micropipette aspiration technique on adult murine valve leaflets (Krishnamurthy et al., 2011). As seen in Fig. 4, control ($Tie1^{fl/fl}$) AoVs were approximately 5-fold stiffer than *Tie1-cko* valves. Thickening and stiffness of heart valves may impair their function and lead to heart valve insufficiency and/or stenosis. Therefore, left side heart function was assessed by echocardiography on control and *Tie1-cko* mice. First, *in utero*, 2D and Doppler echocardiography was performed on prenatal mice. At E17.5 (n=44), embryonic cardiac structure and function, including chamber sizes, systolic volume, ejection fraction, fractional shortening and left ventricle mass were assessed, and we detected no differences between control and *Tie1* mutant animals prior to birth. In addition, the annulus dimensions of both aortic and pulmonary valves were unchanged without evidence of either stenosis or insufficiency (data not shown) when compared with controls. These observations were consistent with the absence of detectable morphological differences prior to birth as described above. However, 2D and Doppler echocardiography performed on 10-week old control and *Tie1-cko* mice demonstrated that 100% of the mutant AoVs showed some degree of aortic regurgitation documented by Doppler (Fig. 5). No AoV or PV insufficiency in control animals was detected. In addition, while there was no change in heart rate of *Tie1-cko* mice compared to control, the mutant hearts showed significant changes in ejection fraction, fractional shortening and a trend towards an increase in left ventricle mass, consistent with aortic valvular insufficiency (Table 2). Taken together, these findings are consistent with our observation that abnormal morphology was only detected in the perinatal and postnatal period.

3.4. *Tie1 attenuation in the valvular endocardium leads to enhanced Sox9 expression and abnormal ECM deposition and organization*

Although *Tie1-cko* mice have a phenotype characterized by AoV

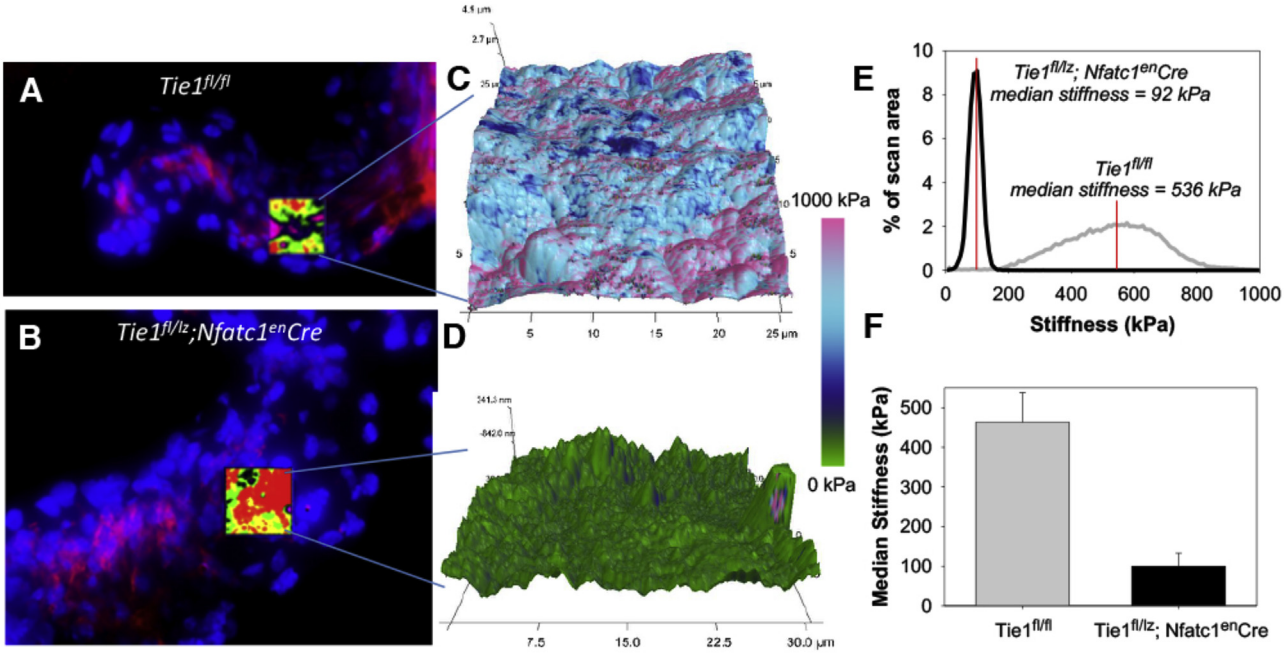

Fig. 4. Tie1 attenuation leads to AoV reduced stiffness. **A,B**, Two channel fluorescence images (blue: nuclei and red: aSMA) of leaflet sections for each group overlaid with the AFM height channel. **C,D**, Stiffness values overlaid on 3D topographical maps that correspond to scanned regions in fluorescent images. **E**, Modulus distributions of AV leaflet AFM scans from *Tie1fl/lz;Nfatc1enCre* and *Tie1fl/fl* mice. Drawn vertical lines represent median modulus values, which are aggregated and plotted in (**F**). AV leaflets from *Tie1fl/fl* mice were significantly stiffer ($p < 0.001$) than *Tie1fl/lz;Nfatc1enCre* valve leaflets.

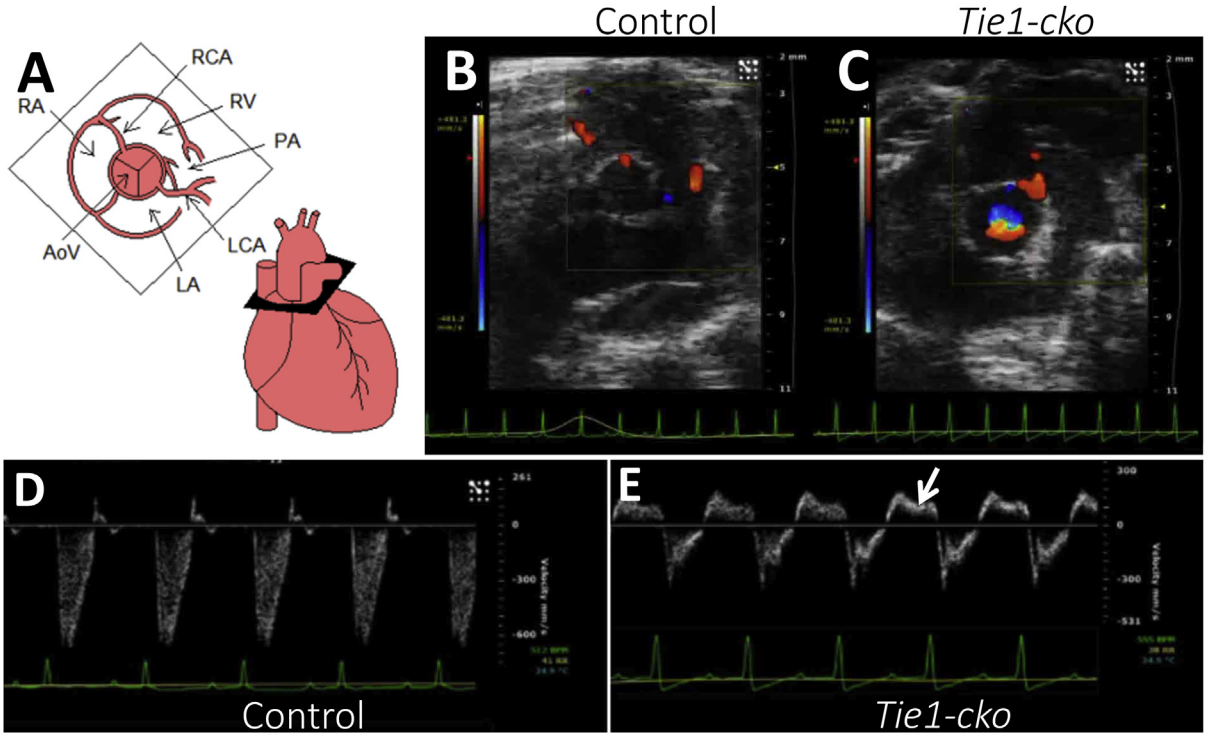

Fig. 5. *Tie1* attenuation leads to AoV insufficiency. **A**, Transverse depiction of the AoV. **B** and **C**, Control and *Tie1-cko* AoVs. Unidirectional blood flow, detected by color flow Doppler, is detected during systole (red), and moderate central aortic insufficiency is detected during diastole (blue, **C**). Doppler profile of control (**D**) and *Tie1-cko* AoVs (**E**) identifying holodiastolic aortic insufficiency (arrows).

enlargement, we detected no significant difference on the overall cell number in the valves between *Tie1-cko* and their control littermates from E14.5 to P10 as determined by counting cell nuclei in DAPI-stained AoV sections (Fig. S4). In addition, we detected no significant difference on cell proliferation between *Tie1* mutants and their controls by quantifying the number of proliferating mesenchymal cells in AoVs and PVs by either

Table 2
Echocardiogram statistics for control and *Tie1-cko* adult mice. Measurements taken from 10-week old female control (n=3) and Tie1-cko mice (n=5). The aortic valve measurement describes the annulus dimension as viewed by transthoracic echocardiogram in the parasternal long axis view. P values were calculated using an unpaired, 2-tailed Student's t-test represented as mean ± SD.

Parameters	Control	Tie1-cko	P value
Heart Rate (bpm)	502 ± 27.4	494 ± 15.7	0.62
Vol Syst (mm^3)	17.4 ± 8.5	26.04 ± 7.1	0.14
Vol Diast (mm^3)	50.6 ± 16.7	62.3 ± 10.9	0.27
Ejection Fraction (%)	67 ± 7	57.8 ± 4	0.05
Fractional Shortening (%)	36 ± 5	30.4± 2	0.05
LV Mass-corrected (mg)	60.1 ± 1	68.2 ± 5.1	0.06
AoV annular diameter (mm)	1.07 ± 0.06	1.20 ± 0.13	0.17
Ao Root (mm)	1.48 ± 0.06	1.67 ± 0.11*	0.04
Ao Valve Peak Velocity (mm/sec)	749.3 ± 103.3	876.8 ± 125.65	0.19
Ao Valve Peak Gradient (mmHg)	3 ± 1.01	2.94 ±0.98	0.94

pHH3 immunohistochemistery (E12.5, E14.5, E16.5 and P0, data not shown) or BrdU incorporation assay (E16.5 and E18.5, Fig. S5). Our apoptosis analysis with TUNEL assay or cleaved Cas3 immunostaining detected no difference in endothelial or valvular mesenchymal cell apoptosis between *Tie1* mutants and their control littermates examined at any stage (E14.5, E16.5 and P0, data not shown). Therefore, the increase in AoV size in *Tie1* mutants is unlikely the result of increased cellularity.

Next, ultrastructural analysis of the valve leaflets with transmission EM revealed normal morphology of endothelial cells in the *Tie1* mutant valve leaflets (Fig. S6). To further examine endothelial integrity in *Tie1-cko* valves and to identify the potential downstream targets of Tie1 signaling during remodeling of semilunar valves, we performed immunostaining for Cdh5, CD31, and Tie2, which detected no alterations on the expression of these flow sensitive endothelial markers in *Tie1-cko* hearts from E14.5 to P0 (Fig. S7 and data not shown), indicating that they are unlikely the downstream targets of Tie1 signaling. Similarly, endothelial Fox2 expression, which is normally restricted to the arterial valve

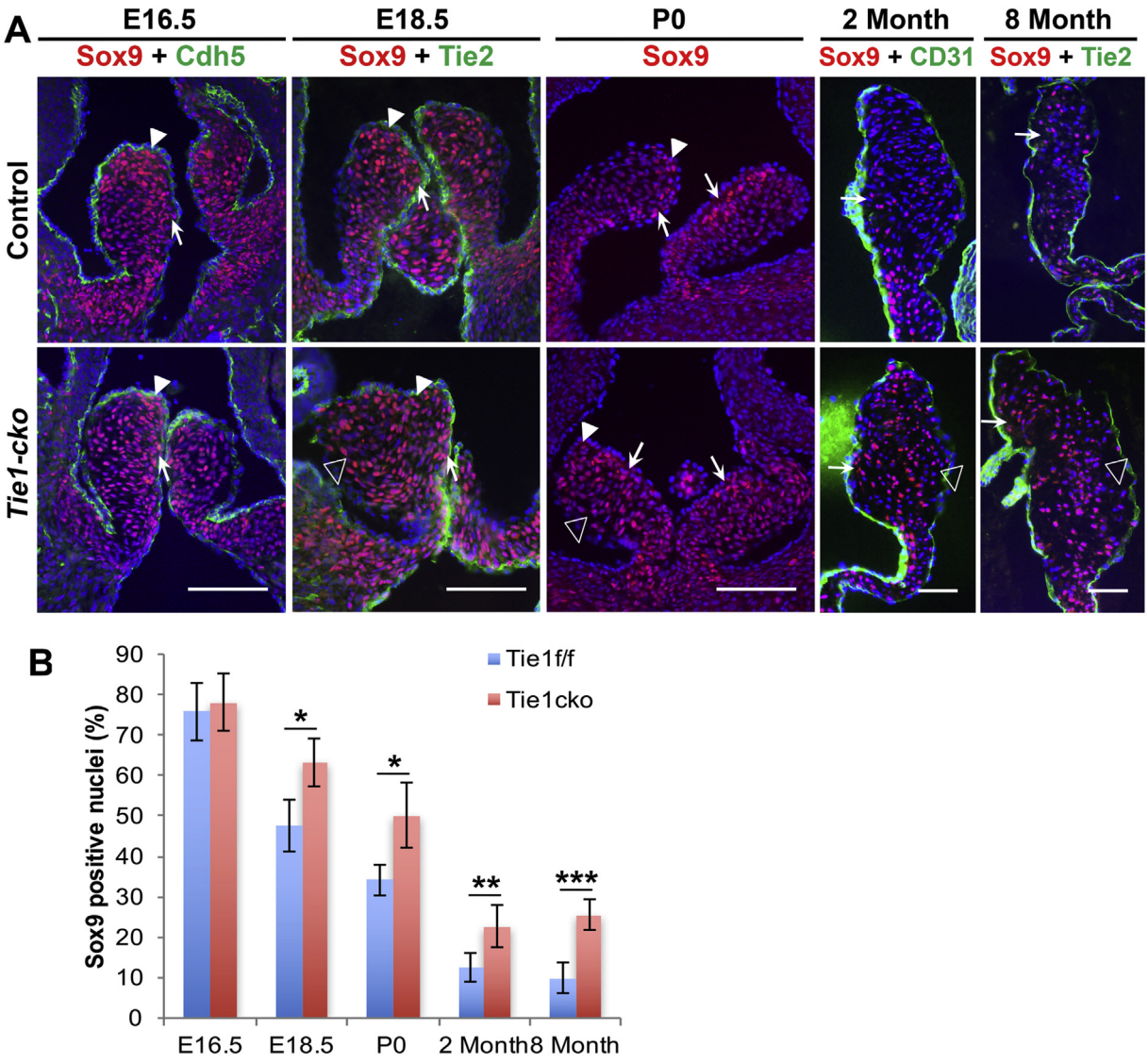

Fig. 6. Tie1 attenuation leads to increased nuclear Sox9 expression in aortic valves. **A**, Representative images of immuno-staining of control and *Tie1-cko* AoVs with anti-Sox9 antibody showing nuclear Sox9 expression (red) at E16.5, E18.5, P0, 2 months and 8 months. These sections were co-stained for Cdh5 (E16.5, green), Tie2 (E18.5 and 8 months, green) or CD31 (2 months, green). In the control, nuclear Sox9 expression is detected throughout valve leaflets at E16.5, then decreases with time, with relatively enhanced expression on the ventricular side (arrows) and the distal tips (arrowheads). The ventricular sides of valve leaflets at 2 months and 8 months are to the left. Compared to the control, Sox9 expression is observed more broadly in *Tie1-cko* valve leaflets and is significantly increased on the arterial side (open arrowheads) from E18.5 to aged mice. Scale bars, 50 μm. **B**, The number of Sox9 positive cells/total nuclei was quantified in AoV leaflet sections. *$P < 0.05$, **$P < 0.01$, ***$P < 0.001$.

surface of the remodeling semilunar valves, was not altered in*Tie1* mutant animals (Fig. S7B).

However, Sox9 expression was surprisingly altered in *Tie1* mutant valves. Expression of Sox9, a SRY transcription factor, is essential for proliferation and ECM maturation during heart valve development (Lincoln et al., 2007). During valvular development, nuclear Sox9 is widely and initially highly expressed in undifferentiated mesenchyme throughout AoV leaflets at early stages, and expression gradually decreases during valve remodeling and maturation (Fig. 6A). Up to E16.5, there was no difference of nuclear Sox9 expression detected between AoVs of *Tie1-cko* and control mice. However, differences in Sox9 expression levels were detected from E18.5 and subsequent stages of development. While Sox9 expression was accentuated on the ventricular side (Fig. 6A, arrows) and the distal tips (arrowheads) of the control AoVs, it was more ubiquitously expressed in *Tie1-cko* valve leaflets and failed to be developmentally down-regulated as in control animals. Strikingly, compared to controls, nuclear Sox9 expression in AoV leaflets of *Tie1* mutant mice was increased by 2 times and 2.5 times at 2-month and 8-month old age, respectively (Fig. 6B).

Consistent with alterations in Sox9 expression, we detected significant alterations in the ECM in *Tie1* mutant aortic valves. Movat's Pentachrome stain, which allows the visualization of organization of collagen, elastin and proteoglycans/glycosaminoglycans (GAGs) together in one colorimetric assay, revealed an increase in GAG content in the valve interstitium of adult (2 months) *Tie1-cko* mice compared to control animals (Fig. 7A). No abnormalities in elastin deposition or

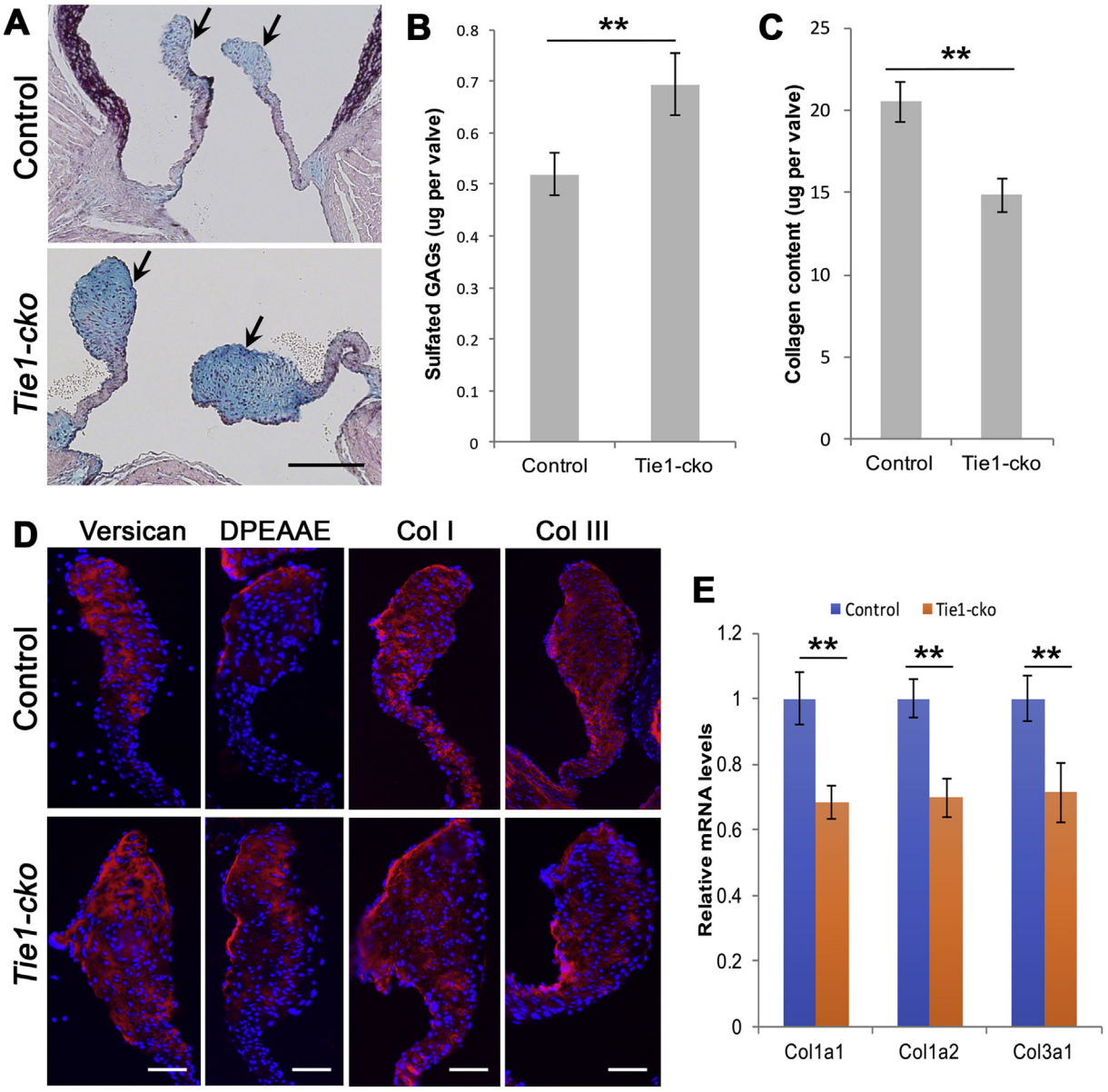

Fig. 7. Tie1 attenuation leads to abnormal ECM deposition and organization. **A,** Movat's Pentachrome stain shows that GAGs deposition (blue) appears to be increased in *Tie1-cko* AoVs as compared to the controls at 2 months. Arrows indicate valve leaflets. Scale bars: 100 μm. **B**, A Sulfated Glycosoaminoglycan (GAG) colormetric assay was utilized to quantify the total GAGs concentrations in control and *Tie1-cko* valves. **C**, Total collagen from control and *Tie1-cko* AoVs was measured using Sircol Soluble Collagen Assay. $^{**}P < 0.01$. **D**, Immunofluorescence staining with antibodies against intact versican, the versican cleaved fragment DPEAAE, Col I and Col III was used to show ECM protein expression in AoV leaflets of 2-month old control and *Tie1-cko* mice. The ventricular sides of valve leaflets are to the left. Scale bars: 50 μm. **E**, qRT-PCR was performed from isolated AoVs of P2 control and *Tie1-cko* mice. This analysis demonstrates significantly decreased changes in expression level of *Col1a1*, *Col1a2*, and *Col3a1* genes in *Tie1-cko* vs. control AoV. $^{**}P < 0.01$.

organization were detected using this method. To quantify the total GAG concentration in adult valves, a sulfated GAG colormetric assay was utilized. A significant increase (33.5%) in GAGs content was detected in *Tie1-cko* AoV as compared to control (Fig. 7B). Coinciding with the increase in GAG content, we observed a decrease in total collagen content in the mutant AoVs. Quantification of total collagen from control and *Tie1-cko* valves was measured using Sircol Soluble Collagen Assay and demonstrated a significant decrease (27.6%) in the amount of collagen in AoV leaflets of *Tie1-cko* animals (Fig. 7C). We further used immunohistochemistry analysis to examine expression patterns of certain critical valvular ECM components. Consistent with Movat's Pentachrome stain and the sulfated GAG colormetric assay, *Tie1-cko* AoV leaflets at P2, 2 months and 8 months appear to exhibit increased expression of hyaluronan (using biotinylated hyaluronic acid binding protein, HABP) and intact versican (using anti-GAGβ, versican antibody), although there was no clear alteration in the distribution of expression between *Tie1-cko* and control (Fig. 7D, S8 and data not shown). However, the versican cleaved fragment DPEAAE which normally becomes restricted in the tip of control AoV leaflets (on the ventricular side), demonstrated an expanded distribution of expression, including expression on the arterial side of the valve leaflet in *Tie1-cko* AoV at 2 months and 8 months when compared to control AoV valves (Fig. 6D, S8B). Immunostaining also revealed a decreased Col I and Col III expression in *Tie1-cko* AoV at P2, 2 months and 8 months, along with reduction of *Col1a1*, *Col1a2* and *Col3a1* mRNA expression relative to controls at P2 (Fig. 7E). Thus, *Tie1* attenuation leads to abnormal postnatal ECM remodeling evident in increased proteoglycan expression and decreased fibrillar collagen expression, consistent with abnormal valve remodeling.

4. Discussion

Responses of valve endothelial cells to shear stress forces generated by blood flow are believed to be important for valve development. However, how VECs respond to hemodynamic forces, particularly disturbed flow, to regulate heart valve remodeling, is not well understood. In the present study, we show that valvular endothelial Tie1 and other EC markers (Cdh5, CD31 and Tie2) are expressed in a dynamic pattern predicted by hemodynamic shear forces during valve remodeling. We demonstrate that Tie1 is restricted to regions of disturbed flow during semilunar valve maturation and is an essential component of valve remodeling. Loss of Tie1 in valve endothelium results in thickened valves that have abnormal ECM organization and deposition, leading to decreased valve stiffness and functional insufficiency that is primarily detected in the aortic valves of perinatal and postnatal mice. Concurrently, Tie1 attenuation in the valvular endocardium leads to enhanced Sox9 expression in VICs, which plays a key role in modulating normal ECM patterning during valve remodeling. Thus, these results suggest that Tie1 acts as a hemodynamic sensor in the valve leaflet and plays a role in crosstalk between the endothelium and the mesenchyme to relay spatial and temporal information during valve remodeling.

In mammals, four main types of valves (cardiac valves, venous valves, lymphatic valves and lymphovenous valves) form to regulate the unidirectional flow of fluid in different organs. Intriguing similarities have recently emerged between the different types of valves concerning their molecular identity, architecture and development that suggest they share conserved mechanisms during normal development. Experimental models have recently been developed, delineating the importance of shear forces in regulation of the expression of genes that are necessary for vascular valve development (review in Geng et al., 2017), and these genes are also expressed in the aortic valves, thus revealing a previously unanticipated commonality between the aortic valves and vascular valves. Elegant studies demonstrated that oscillatory shear stress up-regulates the expression of FOXC2, GATA2, CX37, ephrin-B2 and ITGA9 in lymphatic ECs (Sabine et al., 2012; Geng et al., 2017; Cha et al., 2016) and is the initial regulator of lymphatic valve specification. Tie1 can regulate cellular responses to disturbed blood flow in the arterial circulation (Woo et al., 2011) and is a critical component in regulating the lymphatic valve development that is initiated by disturbed flow (Qu et al., 2015). However, how oscillatory shear stress would affect development of cardiac valves is poorly understood. As mentioned previously, in aortic valves, endothelial cells experience position-dependent differences in hemodynamic shear stress. High laminar shear stress vs. oscillatory shear stress confers distinct molecular profiles in endothelial cells on the ventricular and arterial sides of aortic valves, respectively. For example, expression of EC markers such as Klf2, Klf4 and CX43, enriched on the ventricular side of the cardiac valves, is up-regulated by laminar shear stress (Gitler et al., 2003; Inai et al., 2004; Simmons et al., 2005; Goddard et al., 2017). In contrast, the expression of Foxc2, ephrin-B2 and CX37 in endothelial cells on the downstream or arterial side is activated by oscillatory shear stress (Gitler et al., 2003; Cowan et al., 2004; Inai et al., 2004). We demonstrate that Tie1 is expressed almost equally in the endothelial cells on ventricular and arterial surfaces of the semilunar valves until E14.5. However, as the endocardial cushions become excavated from the aortic side inward during leaflet formation, the aortic sides of AoV are predicted to face increasingly disturbed shear forces (van der Linde et al., 2011). Accordingly, endothelial Tie1 and Cdh5 start (E16.5-E18.5) to exhibit higher expression on the arterial side than on the ventricular side (predicted to face higher laminar shear forces). Attenuated Tie1 expression during this period of development results in a thickened AoV phenotype in *Tie1* mutant mice and in alterations of Sox9 expression in mesenchymal cells of *Tie1* mutant AoVs. We did observe occasional sporadic expression of Tie1 on the ventricular surface of the postnatal valve endocardium, though expression on the arterial side was uniform and significantly higher than that seen on the ventricular side of the leaflet. Nonetheless, we cannot rule out that low level, deletion of Tie1 on the ventricular cusp could have at least partially contributed to the phenotype observed.

Sox9 is predominantly expressed throughout all stages of valvulogenesis. Previous studies suggest that Sox9 is required not only early in valve development, for expansion of the precursor cell population, modulating the expression of key transcription factors required for heart valve development (Garside et al., 2015), but also later for normal expression and distribution of valvular ECM proteins, and its expression in VICs is tightly regulated during normal heart valve development. When the floxed *Sox9* allele was inactivated only in EC derivatives that make up the EC using *Tie2-Cre*, the mutant mice die before E14.5 with hypoplastic ECs, reduced cell proliferation and altered extracellular matrix protein (ECM) deposition (Lincoln et al., 2007). Later inactivation of Sox9 with *Col2a1-Cre* (predominantly in differentiating cartilage cell lineages on the downstream side of valve leaflets) results in perinatal death with thickened heart valve leaflets, and abnormal ECM patterning. Thickened valve leaflets and abnormal ECM production are even observed in adult mice with *Col2a1-Cre* mediated heterozygous loss of *Sox9* suggesting that *Sox9* also regulates ECM organization and homeostasis in adult heart valves. An unpublished work from Dr. Lincoln's lab (Lein et al., 2019) utilized CDH5-CreER and Sox9-HPRT transgenic mice to overexpress Sox9 in VECs at post-natal days 2–4 by administering tamoxifen. At 10 weeks of age, these mice have thickened aortic valves characterized by an abnormal abundance of proteoglycans. Consistent with these observations, *Tie1-cko* mice demonstrate dramatic alteration of nuclear Sox9 expression and develop abnormal ECM remodeling. This suggests that endothelial-mesenchymal signaling thought to be essential in valve remodeling is at least partially mediated by a Tie1-Sox9 paracrine signaling in response to hemodynamic sheer stress.

It is intriguing that loss of *Tie1* leads to abnormal postnatal ECM remodeling characterized by an in increase in proteoglycan expression and decrease in fibrillar collagen expression. In fact, ECM organization and homeostasis of mature heart valves are also affected by hemodynamic environment. The effect of laminar and oscillatory shear stress on the production of collagen and GAGs has been studied in the porcine AoV leaflets *ex vivo*. These studies show that the response of ECs from the aortic side of the valve have a unique capability to respond to oscillatory

flow with increased collagen expression that is not seen by ECs from the ventricular surface (Balachandran et al., 2009; Mongkoldhumrongkul et al., 2018). Our studies suggest that this capability is perturbed, *in vivo*, following attenuation of Tie1.

The penetrance of the AoV enlargement phenotype in adult *Tie1-cko* mice is only about 70% instead of 100%. This is likely the result of variable efficiency of Tie1 deletion mediated by *Nfatc1^{en}Cre*. Interestingly, structure and function of the aortic valve were affected more than that of the pulmonary valve. We have previously documented unique protein expression profiles that distinguish the mature aortic and pulmonary valve leaflets (Angel et al., 2011); therefore, it is not unexpected that the aortic valve would be preferentially affected by *Tie1* deletion in the endocardium. It is possible that these studies reveal an enhanced intrinsic capability of aortic valve VIC cell population to promote matrix remodeling in response to endothelial signaling compared to pulmonary VICs, which would be predicted from *in vitro* studies (Merryman et al., 2006; Gupta et al., 2009). However, the fact that no significant changes were observed until the perinatal and postnatal period, despite attenuation of Tie1 expression in early development, suggests that important factors, other than intrinsic differences between the aortic and pulmonary valve, play a role in the phenotype observed. This can be at least partially explained by the impact of hemodynamic changes imposed as a result of the transitional circulation at birth, where an abrupt decrease in pulmonary resistance and concomitant increase in systemic vascular resistance occurs with loss of the low resistance placental circulation and ductal closure (reviewed in Noori et al., 2012). These hemodynamic changes result in exposure of the AoV leaflets to an increase in strain compared to that experienced by the PV leaflets. Cyclic strain has been shown to reduce total GAG content (Gupta et al., 2009) and increase the collagen content (Balachandran et al., 2006) of AoV leaflets *in vitro*, and AoVs have clearly been shown to demonstrate increased stiffness and collagen biosynthesis compared to PVs (Merryman et al., 2006). In addition, cyclic strain has been shown to increase the expression of Tie1 (Zheng et al., 2004), Tie2 and Ang2 (Chang et al., 2003) in non-valvular endothelial cell populations. Our studies would suggest that Tie1 is at least partially responsible for mediating the effects of aortic valvular strain during perinatal valve morphogenesis. The presence of aortic insufficiency also supports abnormal response to increased valvular strain in the endocardial *Tie1* mutant animals as central component of the phenotype observed.

The alterations in valve mechanical stiffness and functional insufficiency are both consistent with the indices obtained by AFM as well as high resolution ultrasound. One might expect the increased valve size to result in a stiffer and less compliant valve with resultant aortic stenosis. However, decrease in collagen content and increased GAG content resulted in more flaccid and insufficient valves predominately observed on the systemic semilunar valves after birth. This valvular insufficiency was likely a major factor in the late embryonic and perinatal death observed in *Tie1-cko* animals.

In summary, this study provides the first evidence that the RTK Tie1 is involved in modulation of late valve remodeling and suggests that a Tie1-Sox9 signaling axis through which disturbed forces are converted by endocardial cells to paracrine Sox9 signals that modulate the remodeling of AoV. We also confirm that the early postnatal period of AoV development is particularly sensitive to perturbation. Further elucidation of the role of Tie1 in modulating critical processes during this window of development may identify novel pharmacologic therapeutic strategies to help ameliorate congenital valvular disease.

Disclosures

None.

Declarations of interest

None.

Acknowledgements

We would like to thank Dr. Joy Lincoln for sharing her results prior to publication, Dr. Robert Price and members of the University of South Carolina electron microscopy center for assistance with the analysis of valvular endothelial cells, and Alice Qu for drawing the cartoon model of the aortic valve in the graphical abstract. This work was supported by grants from NHLB/NIH: R01HL095255, R01HL118386 (H.S.B.), R01HL094707 (W.D.M.), R01HL118386-S1 (LSJ), and T32 HL007411(KV). LSJ was also supported by NIH T32 GM008554. KV was supported by AHA Pre-doctoral fellowship 12PRE0715381, M.K.S-L was supported as an AHA Pre-doctoral Fellowship 12PRE12070154, and LSJ was supported by AHA Predoctoral Fellowship 12PRE11530015.

Appendix A. Supplementary data

Supplementary data to this article can be found online at https://doi.org/10.1016/j.ydbio.2019.07.011.

References

Aikawa, E., Whittaker, P., Farber, M., Mendelson, K., Padera, R.F., Aikawa, M., Schoen, F.J., 2006. Human semilunar cardiac valve remodeling by activated cells from fetus to adult: implications for postnatal adaptation, pathology, and tissue engineering. Circulation 113, 1344–1352.

Angel, P.M., Nusinow, D., Brown, C.B., Violette, K., Barnett, J.V., Zhang, B., Baldwin, H.S., Caprioli, R.M., 2011. Networked-based characterization of extracellular matrix proteins from adult mouse pulmonary and aortic valves. J. Proteome Res. 10, 812–823.

Balachandran, K., Konduri, S., Sucosky, P., Jo, H., Yoganathan, A.P., 2006. An ex vivo study of the biological properties of porcine aortic valves in response to circumferential cyclic stretch. Ann. Biomed. Eng. 34, 1655–1665.

Balachandran, K., Sucosky, P., Jo, H., Yoganathan, A.P., 2009. Elevated cyclic stretch alters matrix remodeling in aortic valve cusps: implications for degenerative aortic valve disease. Am. J. Physiol. 296, H756–H764, 41.

Cha, B., Geng, X., Mahamud, M.R., Fu, J., Mukherjee, A., Kim, Y., Jho, E.H., Kim, T.H., Kahn, M.L., Xia, L., et al., 2016. Mechanotransduction activates canonical Wnt/beta-catenin signaling to promote lymphatic vascular patterning and the development of lymphatic and lymphovenous valves. Genes Dev. 30, 1454–1469.

Chang, H., Wang, B.W., Kuan, P., Shyu, K.G., 2003. Cyclical mechanical stretch enhances angiopoietin-2 and tie2 receptor expression in cultured human umbilical vein endothelial cells. Clin. Sci. (Lond.) 104, 421–428.

Chiplunkar, A.R., Lung, T.K., Alhashem, Y., Koppenhaver, B.A., Salloum, F.N., Kukreja, R.C., Haar, J.L., Lloyd, J.A., 2013. Kruppel-like factor 2 is required for normal mouse cardiac development. PLoS One 8, e54891.

Cowan, C.A., Yokoyama, N., Saxena, A., Chumley, M.J., Silvany, R.E., Baker, L.A., Srivastava, D., Henkemeyer, M., 2004. Ephrin-B2 reverse signaling is required for axon pathfinding and cardiac valve formation but not early vascular development. Dev. Biol. 271, 263–271.

DeLaughter, D.M., Saint-Jean, L., Baldwin, H.S., Barnett, J.V., 2011. What chick and mouse models have taught us about the role of the endocardium in congenital heart disease. Birth Defects Res. Part A Clin. Mol. Teratol. 91, 511–525.

Dumont, D.J., Fong, G.H., Puri, M.C., Gradwohl, G., Alitalo, K., Breitman, M.L., 1995. Vascularization of the mouse embryo: a study of flk-1, tek, tie, and vascular endothelial growth factor expression during development. Dev. Dynam. 203, 80–92.

Garg, V., Muth, A.N., Ransom, J.F., Schluterman, M.K., Barnes, R., King, I.N., Grossfeld, P.D., Srivastava, D., 2005. Mutations in NOTCH1 cause aortic valve disease. Nature 437, 270–274.

Garside, V.C., Cullum, R., Alder, O., Lu, D.Y., Vander Werff, R., Bilenky, M., Zhao, Y., Jones, S.J., Marra, M.A., Underhill, T.M., Hoodless, P.A., 2015. SOX9 modulates the expression of key transcription factors required for heart valve development. Development 142, 4340–4350.

Geng, X., Cha, B., Mahamud, M.R., Srinivasan, R.S., 2017. Intraluminal valves: development, function and disease. Dis. Model. Mech. 10, 1273–1287.

Gerety, S.S., Wang, H.U., Chen, Z.F., Anderson, D.J., 1999. Symmetrical mutant phenotypes of the receptor EphB4 and its specific transmembrane ligand ephrin-B2 in cardiovascular development. Mol. Cell 4, 403–414.

Gitler, A.D., Lu, M.M., Jiang, Y.Q., Epstein, J.A., Gruber, P.J., 2003. Molecular markers of cardiac endocardial cushion development. Dev. Dynam. 228 (4), 643–650.

Goddard, L.M., Duchemin, A.L., Ramalingan, H., Wu, B., Chen, M., Bamezai, S., Yang, J., Li, L., Morley, M.P., Wang, T., Scherrer-Crosbie, M., Frank, D.B., Engleka, K.A., Jameson, S.C., Morrisey, E.E., Carroll, T.J., Zhou, B., Vermot, J., Kahn, M.L., 2017. Hemodynamic forces sculpt developing heart valves through a KLF2-WNT9B paracrine signaling Axis. Dev. Cell 43 (3), 274–289.

Gupta, V., Tseng, H., Lawrence, B.D., Grande-Allen, K.J., 2009. Effect of cyclic mechanical strain on glycosaminoglycan and proteoglycan synthesis by heart valve cells. Acta Biomater. 5, 531–540.

Hinton Jr., R.B., Lincoln, J., Deutsch, G.H., Osinska, H., Manning, P.B., Benson, D.W., Yutzey, K.E., 2006. Extracellular matrix remodeling and organization in developing and diseased aortic valves. Circ. Res. 98, 1431–1438.

Hinton Jr., R.B., Alfieri, C.M., Witt, S.A., Glascock, B.J., Khoury, P.R., Benson, D.W., Yutzey, K.E., 2008. Mouse heart valve structure and function: echocardiographic and morphometric analyses from the fetus through the aged adult. Am. J. Physiol. Heart Circ. Physiol. 294, H2480–H2488.
Hoffman, J.I., Kaplan, S., 2002. The incidence of congenital heart disease. J. Am. Coll. Cardiol. 39, 1890–1900.
Inai, T., Mancuso, M.R., McDonald, D.M., Kobayashi, J., Nakamura, K., Shibata, Y., 2004. Shear stress-induced upregulation of connexin 43 expression in endothelial cells on upstream surfaces of rat cardiac valves. Histochem. Cell Biol. 122, 477–483.
Krishnamurthy, V.K., Guilak, F., Narmoneva, D.A., Hinton, R.B., 2011. Regional structure-function relationships in mouse aortic valve tissue. J. Biomech. 44, 77–83.
Lein, S., Gallina, D., McDermott, M., Lincoln, J., 2019. Sox9 overexpression in valve endothelial cells causes myxomatous-like valve phenotype. In: Weinstein Cardiovascular Development Conference May 9-11, p. 98 in Indianapolis, IN.
Lin, C.J., Lin, C.Y., Che, C.H., Zhou, B., Chang, C.P., 2012. Partitioning the heart: mechanisms of cardiac septation and valve development. Development 139, 3277–3299.
Lincoln, J., Kist, R., Scherer, G., Yutzey, K.E., 2007. Sox9 is required for precursor cell expansion and extracellular matrix organization during mouse heart valve development. Dev. Biol. 305, 120–132.
Levine, R.A., Hagege, A.A., Judge, D.P., Padala, M., Dal-Bianco, J.P., Aikawa, E., Beaudoin, J., Bischoff, J., Bouatia-Naji, N., Bruneval, P., et al., 2015. Mitral valve disease–morphology and mechanisms. Nat. Rev. Cardiol. 12, 689–710.
Merryman, W.D., Youn, I., Lukoff, H.D., Krueger, P.M., Guilak, F., Hopkins, R.A., Sacks, M.S., 2006. Correlation between heart valve interstitial cell stiffness and transvalvular pressure: implications for collagen biosynthesis. Am. J. Physiol. Heart Circ. Physiol. 290, H224–H231.
Mongkoldhumrongkul, N., Latif, N., Yacoub, M.H., Chester, A.H., 2018. Effect of side-specific valvular shear stress on the content of extracellular matrix in aortic valves. Cardiovasc Eng Technol 9 (2), 151–157.
Noori, S., Wlodaver, A., Gottipati, V., McCoy, M., Schultz, D., Escobedo, M., 2012. Transitional changes in cardiac and cerebral hemodynamics in term neonates at birth. J. Pediatr. 160, 943–948.
Odelin, G., Faure, E., Kober, F., Maurel-Zaffran, C., Théron, A., Coulpier, F., Guillet, B., Bernard, M., Avierinos, J.F., Charnay, P., Topilko, P., Zaffran, S., 2014. Loss of Krox20 results in aortic valve regurgitation and impaired transcriptional activation of fibrillar collagen genes. Cardiovasc. Res. 104, 443–455.
Porat, R.M., Grunewald, M., Globerman, A., Itin, A., Barshtein, G., Alhonen, L., Alitalo, K., Keshet, E., 2004. Specific induction of tie1 promoter by disturbed flow in atherosclerosis-prone vascular niches and flow-obstructing pathologies. Circ. Res. 94, 394–401.
Puri, M.C., Rossant, J., Alitalo, K., Bernstein, A., Partanen, J., 1995. The receptor tyrosine kinase TIE is required for integrity and survival of vascular endothelial cells. EMBO J. 14, 5884–5891.
Qu, X., Tompkins, K., Batts, L.E., Puri, M., Baldwin, S., 2010. Abnormal embryonic lymphatic vessel development in Tie1 hypomorphic mice. Development 137, 1285–1295.
Qu, X., Zhou, B., Baldwin, H.S., 2015. Tie1 is required for lymphatic valve and collecting vessel development. Dev. Biol. 399, 117–128.
Sabine, A., Agalarov, Y., Maby-El Hajjami, H., Jaquet, M., Hä gerling, R., Pollmann, C., Bebber, D., Pfenniger, A., Miura, N., Dormond, O., et al., 2012. Mechanotransduction, PROX1, and FOXC2 cooperate to control connexin37 and calcineurin during lymphatic-valve formation. Dev. Cell 22, 430–445.
Sewell-Loftin, M.K., Brown, C.B., Baldwin, H.S., Merryman, W.D., 2012. Novel technique for quantifying heart valve leaflet stiffness with atomic force micrsocopy. J. Heart Valve Dis. 21, 513–520.
Simmons, C.A., Grant, G.R., Manduchi, E., Davies, P.F., 2005. Spatial heterogeneity of endothelial phenotypes correlates with side-specific vulnerability to calcification in normal porcine aortic valves. Circ. Res. 96 (7), 792–799.
van der Linde, D., Konings, E.E., Slager, M.A., Witsenburg, M., Helbing, W.A., Takkenberg, J.J., Roos-Hesselink, J.W., 2011. Birth prevalence of congenital heart disease worldwide: a systematic review and meta-analysis. J. Am. Coll. Cardiol. 58 (21), 2241–2247.
von Gise, A., Pu, W.T., 2012. Endocardial and epicardial epithelial to mesenchymal transitions in heart development and disease. Circ. Res. 110, 1628–1645.
Woo, K.V., Qu, X., Babaev, V.R., Linton, M.F., Guzman, R.J., Fazio, S., Baldwin, H.S., 2011. Tie1 attenuation reduces murine atherosclerosis in a dose-dependent and shear stress-specific manner. J. Clin. Investig. 121, 1624–1635.
Wu, B., Wang, Y., Lui, W., Langworthy, M., Tompkins, K.L., Hatzopoulos, A.K., Baldwin, H.S., Zhou, B., 2011. Nfatc1 coordinates valve endocardial cell lineage development required for heart valve formation. Circ. Res. 109, 183–192.
Yancopoulos, G.D., Davis, S., Gale, N.W., Rudge, J.S., Wiegand, S.J., Holash, J., 2000. Vascular-specific growth factors and blood vessel formation. Nature 407, 242–248.
Zheng, W., Christensen, L.P., Tomanek, R.J., 2004. Stretch induces upregulation of key tyrosine kinase receptors in microvascular endothelial cells. Am. J. Physiol. Heart Circ. Physiol. 287, H2739–H2745.